AD-A124 023 CHATANIKA RADAR MEASUREMENTS OF THE CONTINUOUS AURORA 1/1
(U) SRI INTERNATIONAL MENLO PARK CA R M ROBINSON
OCT 82 AFGL-TR-82-0297 F19628-81-K-0037

UNCLASSIFIED F/G 4/1 NL

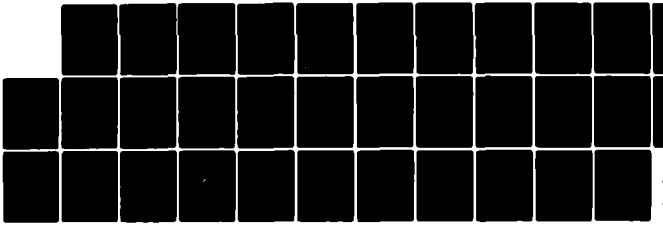

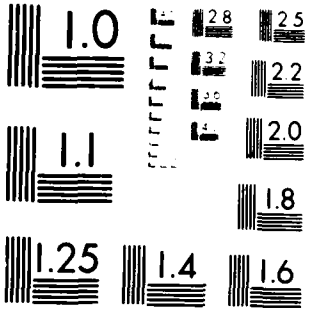

MICROCOPY RESOLUTION TEST CHART

(1.2)

AFGL-TR-82-0297

CHATANIKA RADAR MEASUREMENTS OF THE CONTINUOUS AURORA

Robert M. Robinson

SRI International
333 Ravenswood Avenue
Menlo Park, California 94025

Final Report
Covering the Period 26 January 1981 to 30 September 1982

October 1982

Approved for public release; distribution unlimited.

AIR FORCE GEOPHYSICS LABORATORY
AIR FORCE SYSTEMS COMMAND
UNITED STATES AIR FORCE
HANSCOM AFB, MASSACHUSETTS 01731

UNCLASSIFIED

SECURITY CLASSIFICATION OF THIS PAGE (When Data Entered)

REPORT DOCUMENTATION PAGE		READ INSTRUCTIONS BEFORE COMPLETING FORM
1. REPORT NUMBER AFGL-TR-82-0297	2. GOVT ACCESSION NO A124023	3. RECIPIENT'S CATALOG NUMBER
4. TITLE (and Subtitle) CHATANIKA RADAR MEASUREMENTS OF THE CONTINUOUS AURORA		5. TYPE OF REPORT & PERIOD COVERED Final Report--Covering the Period 26 January 1981 to 30 September 1982
		6. PERFORMING ORG. REPORT NUMBER SRI Project 2734
7. AUTHOR(s) Robert M. Robinson		8. CONTRACT OR GRANT NUMBER(s) F19628-81-K-0037
9. PERFORMING ORGANIZATION NAME AND ADDRESS SRI International 333 Ravenswood Avenue Menlo Park, CA 94025		10. PROGRAM ELEMENT, PROJECT, TASK AREA & WORK UNIT NUMBERS 62101F 464306BC
11. CONTROLLING OFFICE NAME AND ADDRESS Air Force Geophysics Laboratory Hanscom AFB, MA 01731 Monitor/B.S. Dandekar/(PHY)		12. REPORT DATE October 1982 13. NO. OF PAGES 40
14. MONITORING AGENCY NAME & ADDRESS (if diff. from Controlling Office)		15. SECURITY CLASS. (of this report) UNCLASSIFIED 15a. DECLASSIFICATION/DOWNGRADING SCHEDULE

16. DISTRIBUTION STATEMENT (of this report)

Approved for public release; distribution unlimited.

17. DISTRIBUTION STATEMENT (of the abstract entered in Block 20, if different from report)

18. SUPPLEMENTARY NOTES

19. KEY WORDS (Continue on reverse side if necessary and identify by block number)

Diffuse aurora
Continuous aurora
Auroral ionization
Particle precipitation
Electric fields
Chatanika radar

20. ABSTRACT (Continue on reverse side if necessary and identify by block number)

Chatanika radar measurements were made of the continuous aurora during the Air Force Geophysics Laboratory auroral-E rocket launches on 7 March 1981. Four instrumented sounding rockets were launched into the continuous aurora from Poker Flat, Alaska. The radar provided simultaneous measurements of electron density, electric fields, and ion and electron temperatures. The peak E-region densities were between 1 and 2 x 10^5 cm^{-3} at altitudes of 120 to 125 km. The electric field varied between 30 and 50 mV/m. The ion and electron temperatures suggest enhancement from Joule heating. This heating may have caused a higher-

DD FORM 1 JAN 73 1473

EDITION OF 1 NOV 65 IS OBSOLETE

UNCLASSIFIED

SECURITY CLASSIFICATION OF THIS PAGE (When Data Entered)

19 KEY WORDS (Continued)

20 ABSTRACT (Continued)

than-average amount of molecular ions relative to O^+. The ionization in the continuous aurora was produced by precipitating electrons with average energies of about 2 keV and fluxes of 0.5 to 1.5 erg/cm^2 - s. These electrons originated from a Maxwellian source in the plasma sheet with a density of 0.4 cm^{-3} and temperatures varying between 0.8 and 1.6 keV. The radar measurements were reasonably consistent with data from several rocket-borne instruments.

CONTENTS

ILLUSTRATIONS

TABLES

ACKNOWLEDGMENTS

I would like to acknowledge helpful conversations with J. Jasperse (AFGL), R. Vondrak (Lockheed Palo Alto Research Laboratory), and J. Kelly (SRI). D. Walker of Naval Research Laboratory provided plasma probe data. M. Smiddy of AFGL provided rocket electric field data. I would like to thank Mary McCready of SRI for assistance with the radar data processing.

I INTRODUCTION

As part of the Auroral-E Program to study the continuous or diffuse aurora, the Air Force Geophysics Laboratory (AFGL) launched four sounding rockets on the evening of 7 March 1981. The rockets were launched from the Poker Flat Research Range, Alaska and carried instrumentation to measure particle fluxes, optical emissions, ionization, and electric fields, as well as properties of the neutral atmosphere. Coordinated measurements were made by the AFGL Airborne Ionospheric Observatory, the Chatanika radar, and several other ground-based facilities. The primary objective of this experiment was to assess the validity of theoretical models used to deduce ionization profiles from satellite data. The launch criteria for the rocket experiments were based on the requirement that the ionosphere be spatially uniform and that steady conditions exist. The Chatanika radar was operated for nine consecutive nights during the program. The purpose of the radar measurements was twofold:

(1) The real-time data were used to determine if the launch criteria were satisfied.

(2) Postflight analysis of the radar data provides ionospheric information necessary for testing the accuracy of the theoretical models.

In a previous report Robinson and Vondrak (1981)* presented an overview of ionospheric conditions at the time of the experiment. In this report we examine the Chatanika radar data in greater detail. In particular, we describe the radar measurements of ion and electron temperature and discuss the plasma corrections that were applied to the measurements of electron density. We then characterize the precipitating particles producing the ionization in the continuous aurora in terms of the number density and temperature of the source. Finally, we com-

* References are listed in full at the end of this report.

pare the results to those obtained by several rocket-borne instruments: the pulsed-plasma probe, the ion-mass spectrometer, and the electric-field booms.

II EXPERIMENT DESCRIPTION

The four AFGL rockets were launched between 0809 and 0838 UT on 7 March 1981 into a steady auroral E layer. Table 1 lists the instrumentation, flight time, and apogee altitudes of the four payloads. The TMA on Payload 4 was released at 0840 UT. The AFGL aircraft was deployed at 0740 UT and was in flight until about 0930 UT.

Table 2 presents a summary of Chatanika radar operations during the evening of 7 March 1981. The operating modes referred to in the table are described by Robinson and Vondrak (1981). Figure 1 is an electron-density contour plot constructed from radar elevation-scan data obtained just before the rocket launches. The vertical axis is altitude measured along a magnetic flux tube so that field lines are vertical in the plot. The continuous aurora is the broad layer of ionization centered at about 125-km altitude and extending from 64^{o} to 67^{o} invariant latitude. The E-region peak density at this time was 1.4×10^{5} cm^{-3}. Auroral conditions did not change significantly during the four rocket launches. The four payloads penetrated the continuous aurora between 65^{o} and 66^{o} invariant latitude.

Table 1

AURORAL-E ROCKET PAYLOAD AND LAUNCH INFORMATION

Payload	Instrumentation	Flight Time (UT)	Apogee Altitude (km)
(1) A13.030	Electron Proton Spectrometer Six-Channel Photometer Five-Channel VUV Photometer	0809:00 to 0817:52	156.40
(2) A13.020	Mass Spectrometer NRL Pulsed Plasma Probes Electron Density Spectrometer	0809:58 to 0818:27	202.71
(3) A13.031	Electron Proton Spectrometer 2 Spectrometers 1 Photometer	0826:00 to 0834:41	169.66
(4) A10.903	Falling Sphere E-field Booms TMA Release	0838:00 to 0845:16	186.24

Table 2

RADAR OPERATIONS ON 7 MARCH 1981

Time (UT)	Operating Mode	Launch Times
0453 to 0736	Full meridian scans alternated with three-min fixed-position in the magnetic zenith.	
0737 to 0742	Five-min azimuth scan to the east	
0742 to 0755	One full meridian scan	
0756 to 0801	Five-min azimuth scan to the east	
0803 to 0834	Seven partial meridian scans from magnetic zenith to 30° N elevation	0809:00 (A13.030) 0809:58 (A13.020) 0826:00 (A13.031)
0834 to 0849	Switch to multiple-pulse mode	0838:00 (A13.903)
0849 to 0909	Five fixed-position dwells--four-min each. One in magnetic zenith, two at 70° elevation in magnetic meridian and two at 70° elevation in the L shell	
0912 to 0924	One full meridian scan	
0931 to 0939	Two four-min partial meridian scans to the north	
>0939	Meridian scans with fixed position	

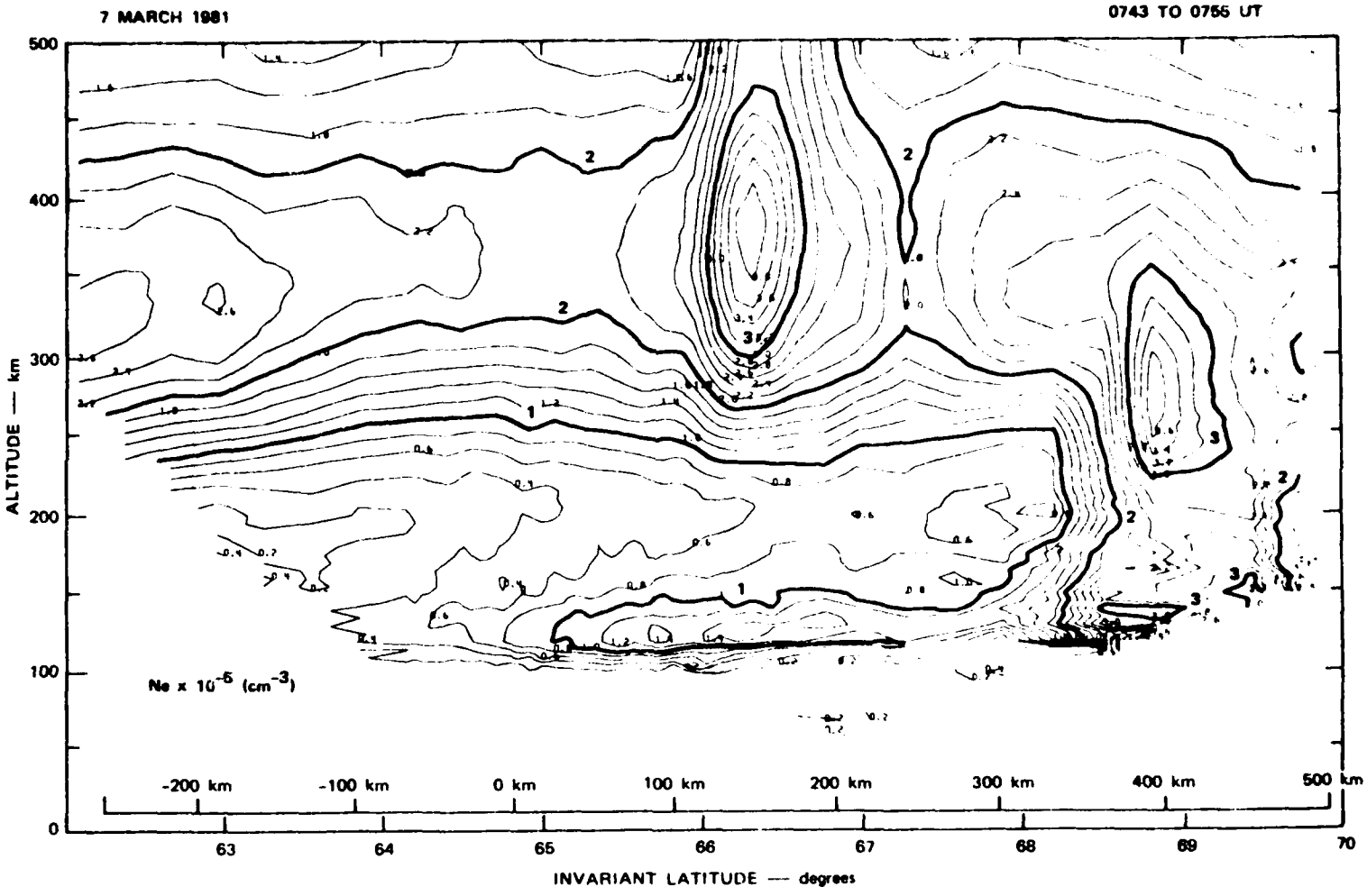

FIGURE 1 ELECTRON-DENSITY CONTOUR PLOT CONSTRUCTED FROM FULL MERIDIAN SCAN 0743 TO 0755 UT. Magnetic field lines are vertical.

III RADAR RESULTS

A. Electron Densities

Figure 2 shows electron density contour plots constructed from radar data obtained during the seven partial elevation scans made during the time of the rocket launches. The electron densities are displayed in a geographic reference frame. The densities shown are raw densities--i.e., temperature corrections have not been applied. The incoherent-backscatter cross section is a function of electron density, electron and ion temperature, and ion mass. Raw densities are computed in the initial phase of data processing using the cold plasma approximations ($T_e = T_i = 0$) and assuming the ion mass given by a model atmosphere. Once the temperature profile has been determined, either by spectral analysis or an independent measurement, these initial density estimates can be corrected. Note that the electron densities shown by Robinson and Vondrak (1981) were corrected using a model temperature profile rather than actual temperature measurements.

Rocket-echo contamination is apparent in several of the contour plots in Figure 1. Because the presence of these echoes makes it impossible to obtain a radar measurement that is spatially and temporally coincident with the rocket measurement, we have chosen five antenna beam positions during the scans to illustrate the range of electron densities measured during the rocket flights. The straight lines in Figures 2(a), 2(c), and 2(d) show the pointing direction of the antenna during the time these measurements were obtained. The data from these measurements are superimposed in Figure 3.

B. Electric Fields

Figure 4 shows the electric field as a function of latitude measured by the radar during the seven elevation scans from 0803 to 0832

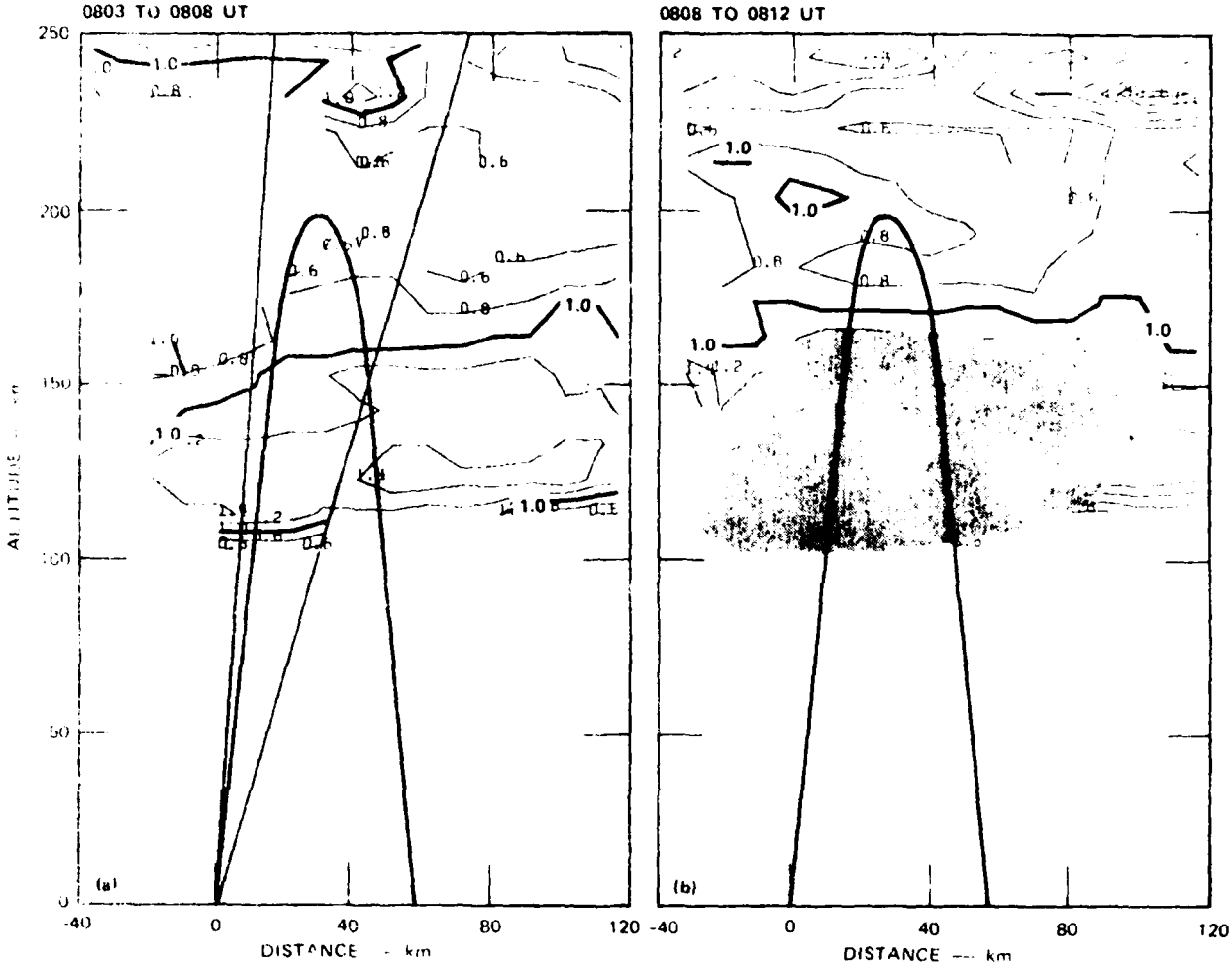

FIGURE 2 ELECTRON-DENSITY CONTOUR PLOTS CONSTRUCTED FROM PARTIAL MERIDIAN SCANS DURING THE FOUR ROCKET LAUNCHES. The trajectory of Payload A13.020 is shown for reference. Shaded areas indicate regions in which rocket echoes contaminated the radar returns. Lines indicate pointing direction of the radar for the data shown in Figure 3. The data are not corrected for plasma effects.

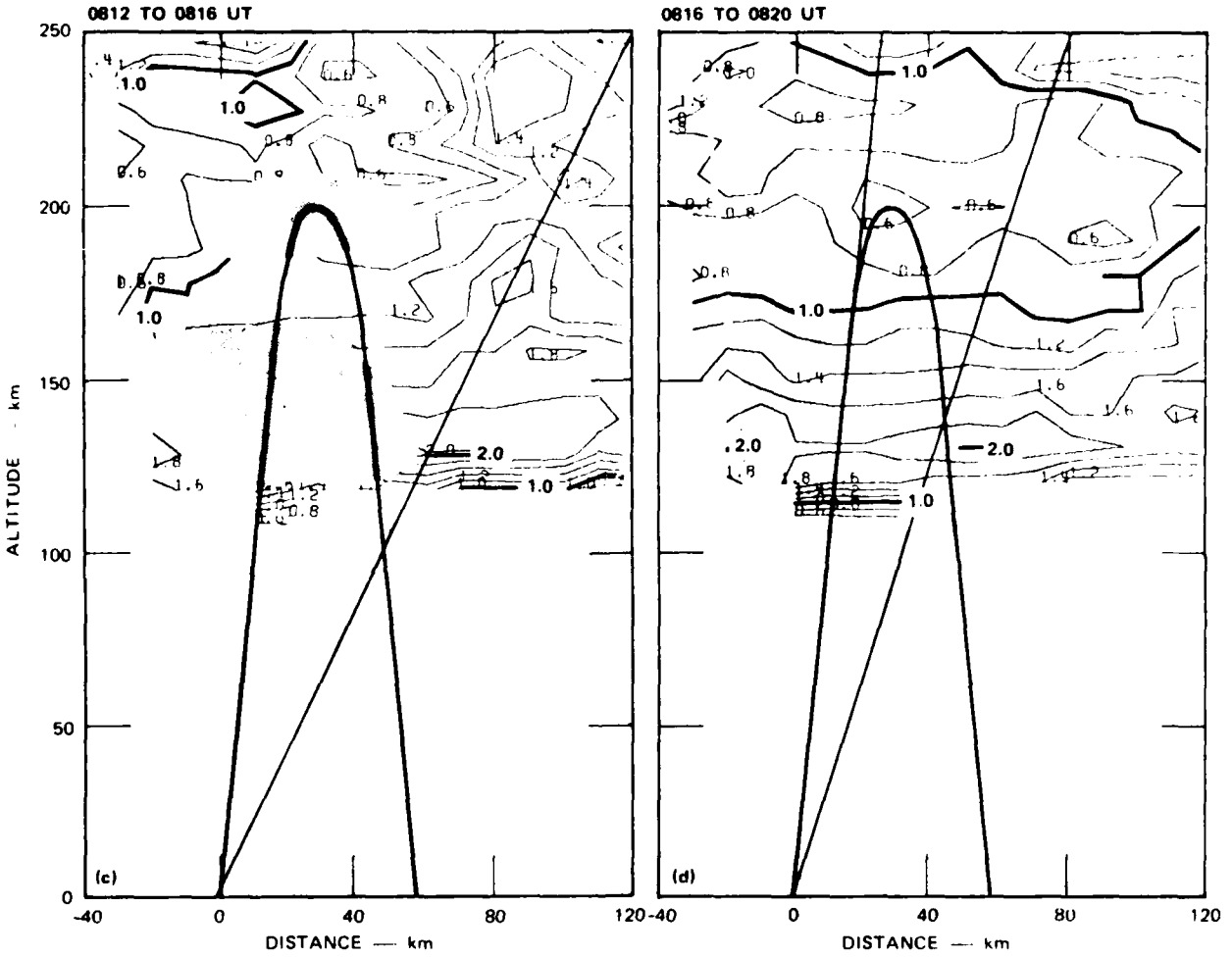

FIGURE 2 (Continued)

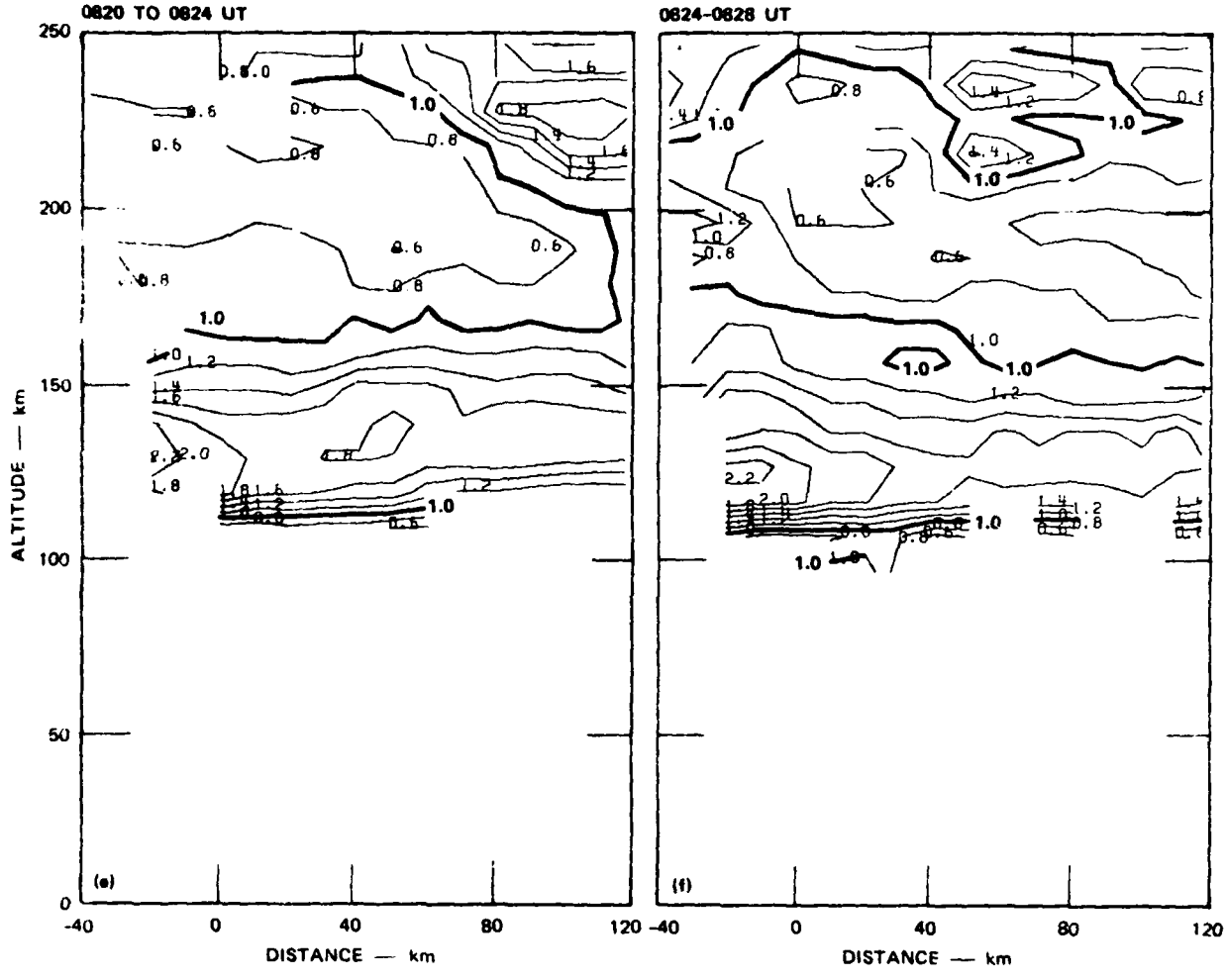

FIGURE 2 (Continued)

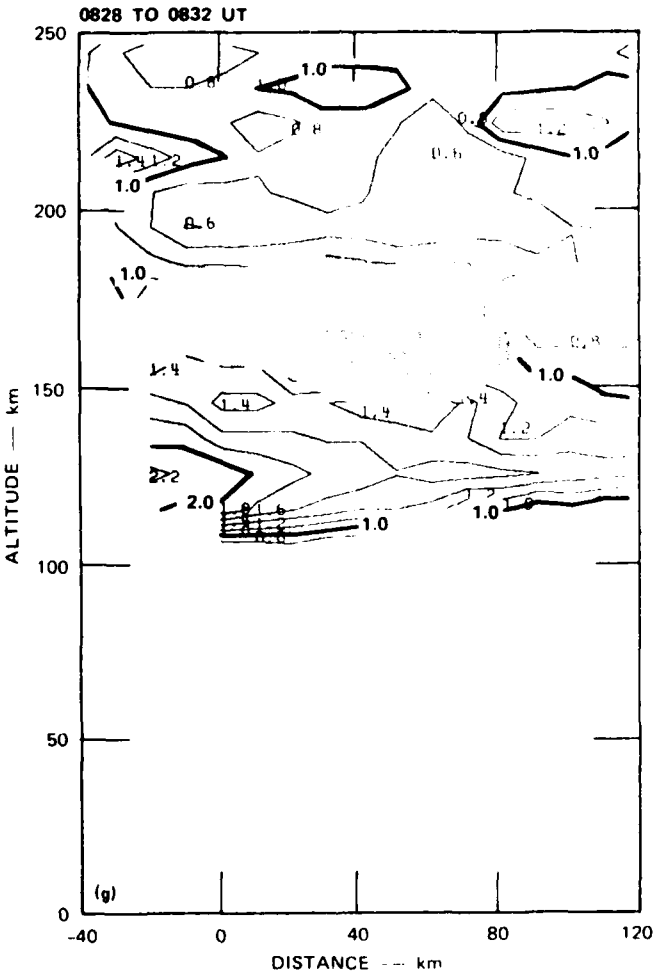

FIGURE 2 (Concluded)

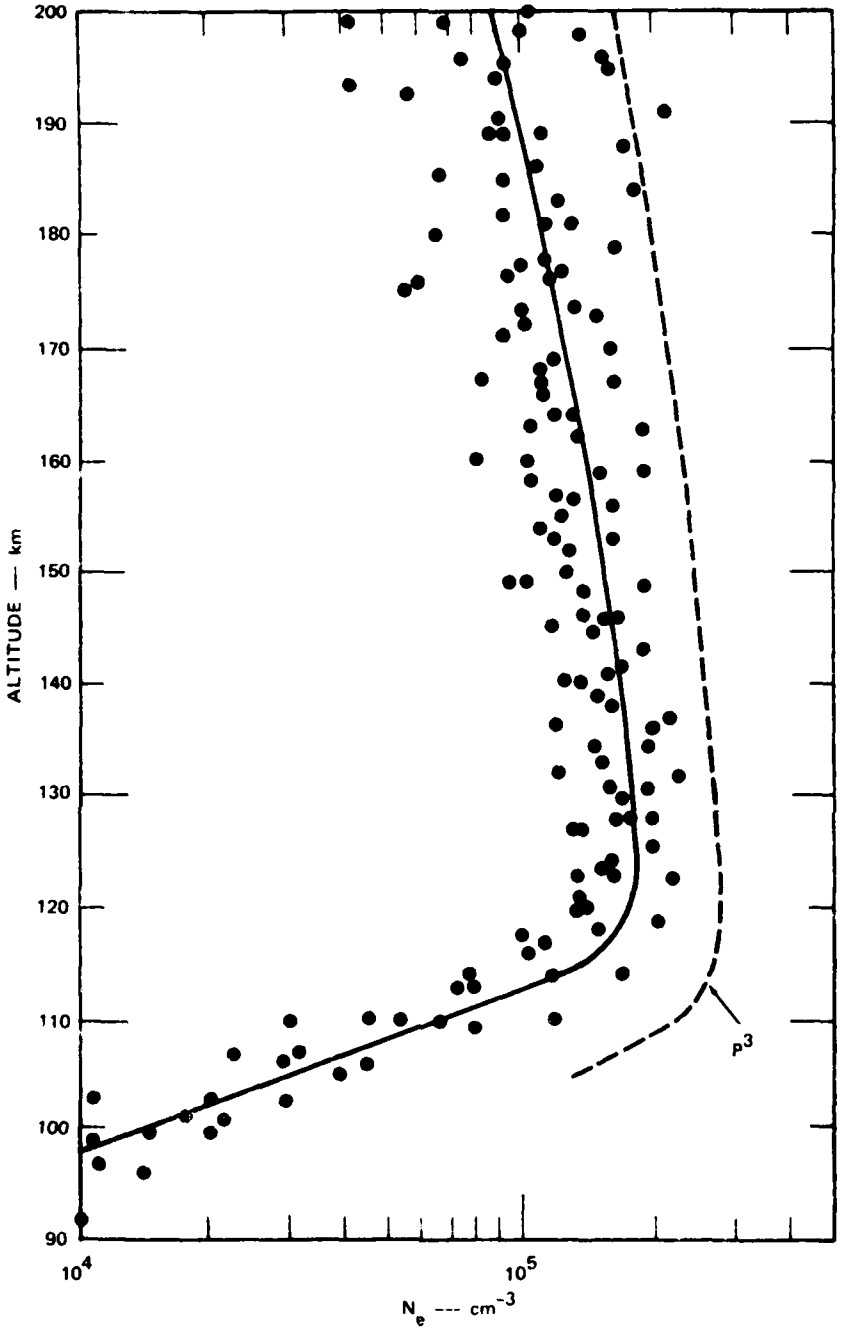

FIGURE 3 RADAR ELECTRON-DENSITY DATA FOR THE FIVE-BEAM POSITIONS SHOWN IN FIGURE 2. The solid curve is an average profile, not meant to indicate an actual profile measured during the experiment. The dashed curve shows the pulsed-plasma-probe (P^3) data obtained on Payload A13.020.

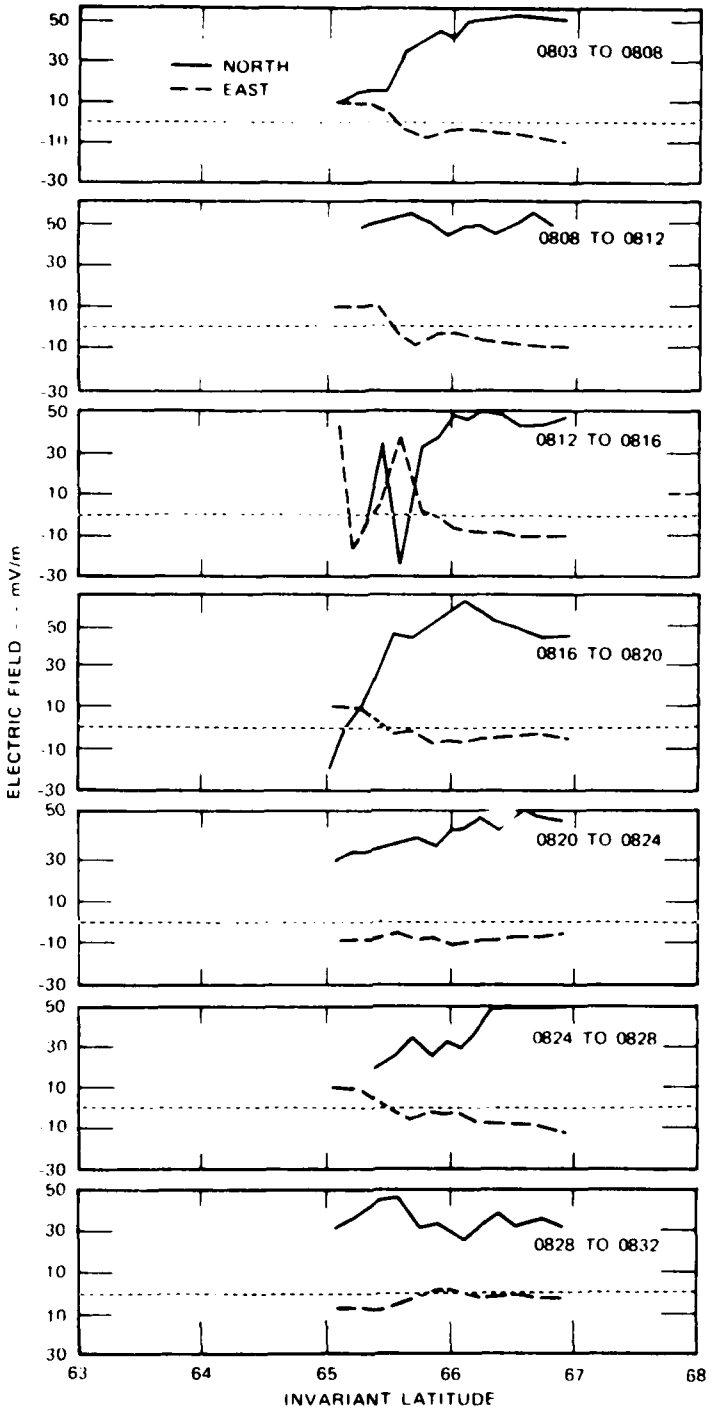

FIGURE 4 **RADAR ELECTRIC-FIELD MEASUREMENTS MADE DURING THE SEVEN PARTIAL MERIDIAN SCANS OF FIGURE 2.** Solid curves are the geomagnetic north components, dashed curves are the geomagnetic east components.

UT. When scanning in the magnetic meridian the radar cannot measure ion drift perpendicular to the meridian plane. The east-west drift (north-south electric field) must be inferred from meridional drift measurements at two different altitudes. One altitude is in the E region and the other is in the F region where the plasma motion results from E x B drift alone. This method assumes that the E-region neutral wind is small. Neglecting the neutral wind, the uncertainty in the north-south electric-field measurement is approximately 5 to 10 mV/m. The uncertainty in the east-west electric field measurement is about 3 mV/m. These uncertainties increase substantially when the antenna is pointing close to the magnetic zenith.

Figure 4 shows that the northward electric field varied between 30 and 50 mV/m during the experiment. The zonal field was about 5 mV/m and was fairly constant with latitude and time. The reversal in the zonal field apparent in several of the scans between 65^{o} and 66^{o} is probably due to the presence of nonzero vertical drifts, which can bias the velocity measurements when the radar is pointing close to the zenith. Note that the geomagnetic northward electric field is slightly smaller in the last two scans than it is in the earlier scans.

C. Temperatures

Radar ion- and electron-temperature measurements were made between 0849 and 0909 UT while the radar was operating in a fixed-position mode. The ion and electron temperatures measured at this time are shown in Figure 5. The radar temperature measurements in the F region are sensitive to the relative abundance of atomic and molecular ions. The transition altitude at which atomic oxygen ions are more abundant than molecular ions depends strongly on auroral conditions, but is generally around 200 km (Kelly and Wickwar, 1981). In computing temperatures from the radar measurements, we have assumed the fractional abundance of O^{+} given by Swider and Narcisi, (1981). These results were obtained from ion-mass-spectrometer data obtained on Payload A13.020.

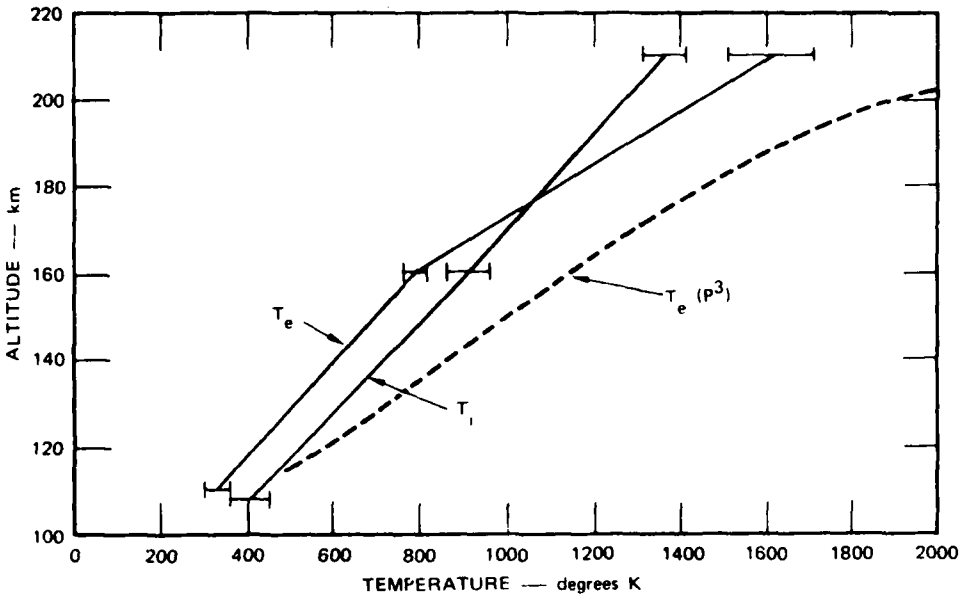

FIGURE 5 RADAR MEASUREMENTS OF ION AND ELECTRON TEMPERATURES MADE BETWEEN 0849 AND 0909 UT. The six measurements are connected by straight line segments. The plasma-probe measurement of electron temperature made about one-half hour earlier is shown for comparison.

D. Corrected Electron Densities

The radar-measured densities shown in Figures 2 and 3 are raw densities. The raw density N_e' is related to the true density N_e according to

$$N_e = \frac{N_e' \ (1 + \alpha^2 + T_r)(1 + \alpha^2)}{2}$$

where

$$\alpha^2 = 14.25 \ T_e/N_e \ (cm^{-3}) \approx 14.25 \ T_e/N_e' \ (cm^{-3})$$

and

$$T_r = T_e/T_i$$

To investigate the effect of temperature on the radar electron density measurements, we have computed the temperature correction using a model temperature profile obtained by linearly interpolating between the points in Figure 5. These profiles are given in Table 3. Also shown in Table 3 is the electron density as a function of altitude given by the solid line in Figure 3. This solid line is not meant to represent an actual electron-density profile measured during the experiment. It is an average profile only used to illustrate the magnitude of the temperature corrections. The last column in Table 3 is the corrected electron density. Both the raw and corrected profiles are plotted in Figure 6.

E. Precipitating Particle Characteristics

Information about the particle precipitation producing the diffuse aurora can be deduced from the electron density profiles. The method has been outlined by Vondrak and Baron (1977). The density profile is converted to a production rate, q(h), according to

$$q(h) = \alpha N_e^2$$

where α is the height-dependent recombination rate and N_e is the electron density. The production profile is deconvolved to yield the flux of electrons as a function of energy between 1 keV and 150 keV. This is done by starting with the lowest altitudes (highest energies) and working upward in altitude (downward in energy). The computed spectra for three selected profiles are plotted on the right hand side of Figures 7 through 9. The solid line is a plot of log F(E) as a function of log E (left hand and upper scales). The dashed line plots the logarithm of the distribution function, F(V), as a function of E (right hand and upper scales). As a check on the calculations, these energy distributions were used to recompute the electron-density profiles (circles in the left hand plots) for comparison with the measured profiles (solid lines on left).

The distribution functions plotted in Figures 7 through 9 are nearly linear because the spectra are Maxwellian. However, in all three figures the distribution functions deviate from pure Maxwellians at an

Table 3

EFFECTS OF PLASMA CORRECTIONS ON RADAR-MEASURED ELECTRON DENSITIES

Altitude (km)	T_e	T_i	$N_e' \times 10^{-5}$ cm^{-3}	$N_e \times 10^{-5}$ cm^{-3}
100	239	303	0.13	0.17
105	285	354	0.3	0.33
110	331	405	0.66	0.67
115	377	456	1.4	1.4
120	423	507	1.8	1.7
125	470	558	1.8	1.8
130	516	609	1.7	1.7
135	562	659	1.7	1.7
140	608	710	1.6	1.6
145	654	762	1.5	1.5
150	701	813	1.5	1.5
155	747	864	1.4	1.5
160	793	913	1.4	1.5
165	876	959	1.3	1.4
170	959	1005	1.2	1.4
175	1041	1051	1.2	1.4
180	1124	1097	1.1	1.4
185	1207	1143	1.0	1.3
190	1290	1188	0.95	1.3
195	1373	1234	0.90	1.3
200	1455	1280	0.85	1.3

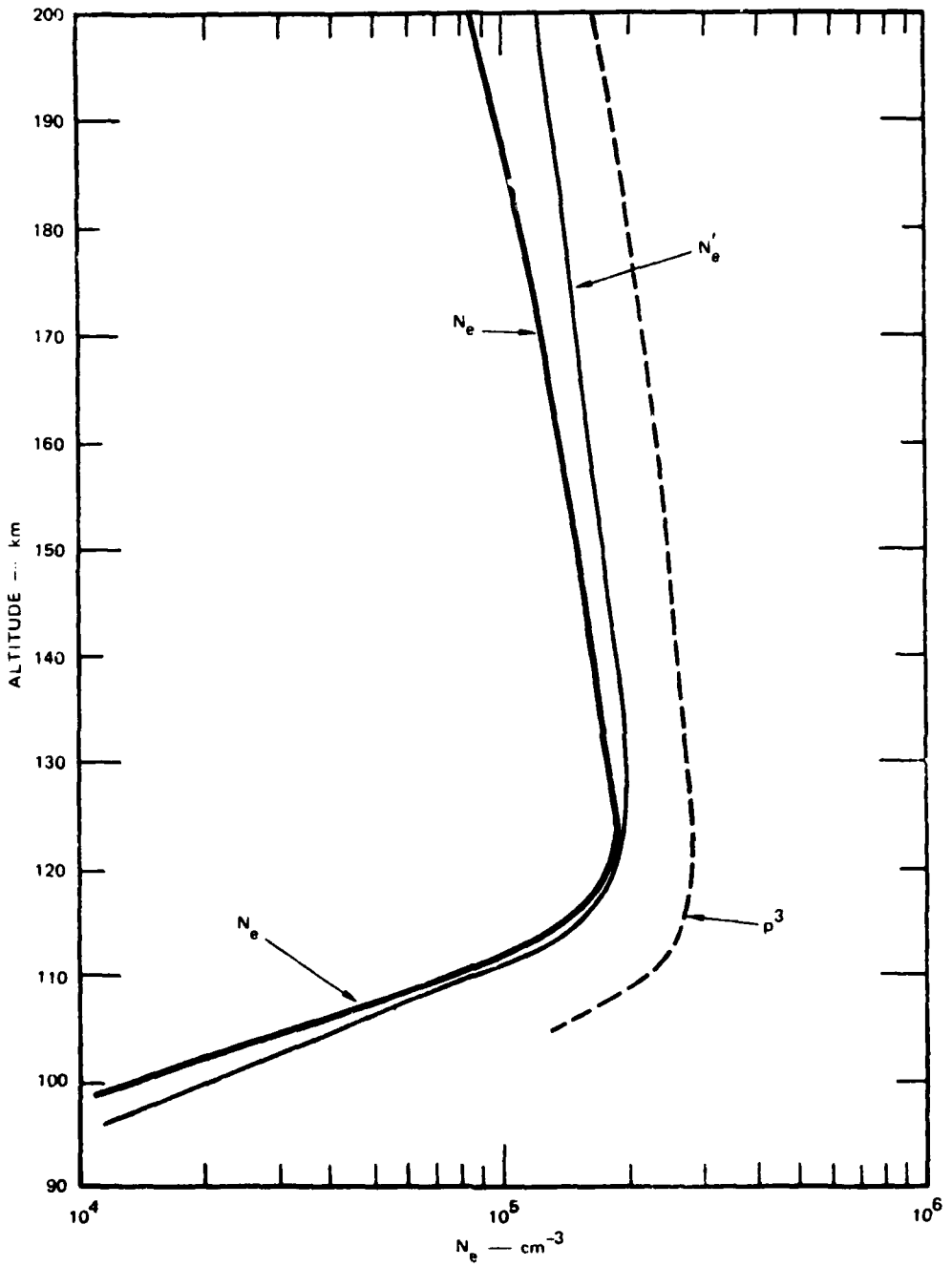

FIGURE 6 EFFECTS OF PLASMA CORRECTIONS ON RAW DENSITY PROFILE. The model temperature profile used is given in Table 3. The heavy curve is the average profile from Figure 3. The thin curve is the corrected profile. The plasma-probe data is shown for comparison.

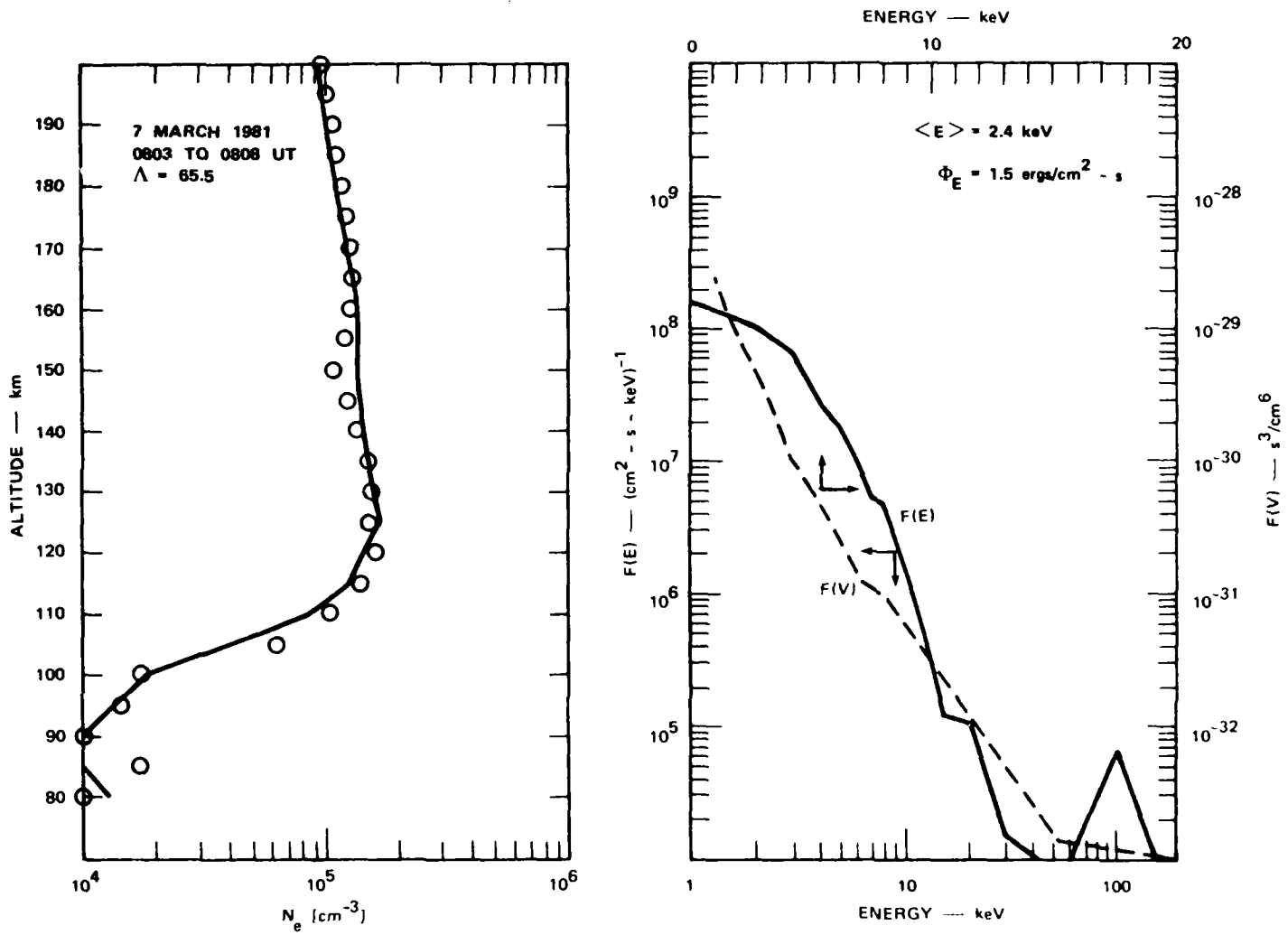

FIGURE 7 ELECTRON-ENERGY SPECTRUM DEDUCED FROM A FIELD-ALIGNED DENSITY PROFILE MEASURED BETWEEN 0803 AND 0808 UT

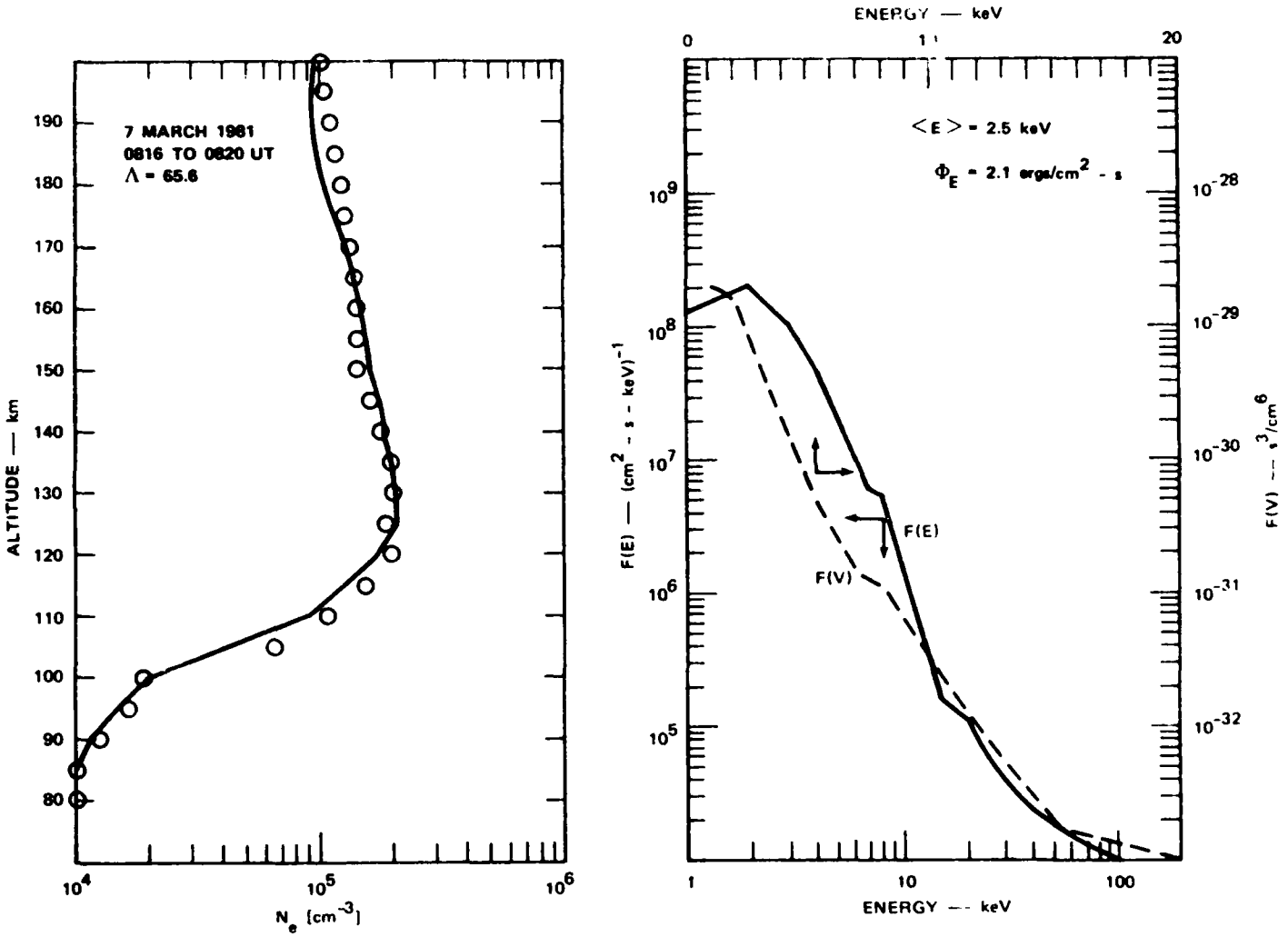

FIGURE 8 ELECTRON-ENERGY SPECTRUM DEDUCED FROM A FIELD-ALIGNED DENSITY PROFILE MEASURED BETWEEN 0816 AND 0820 UT

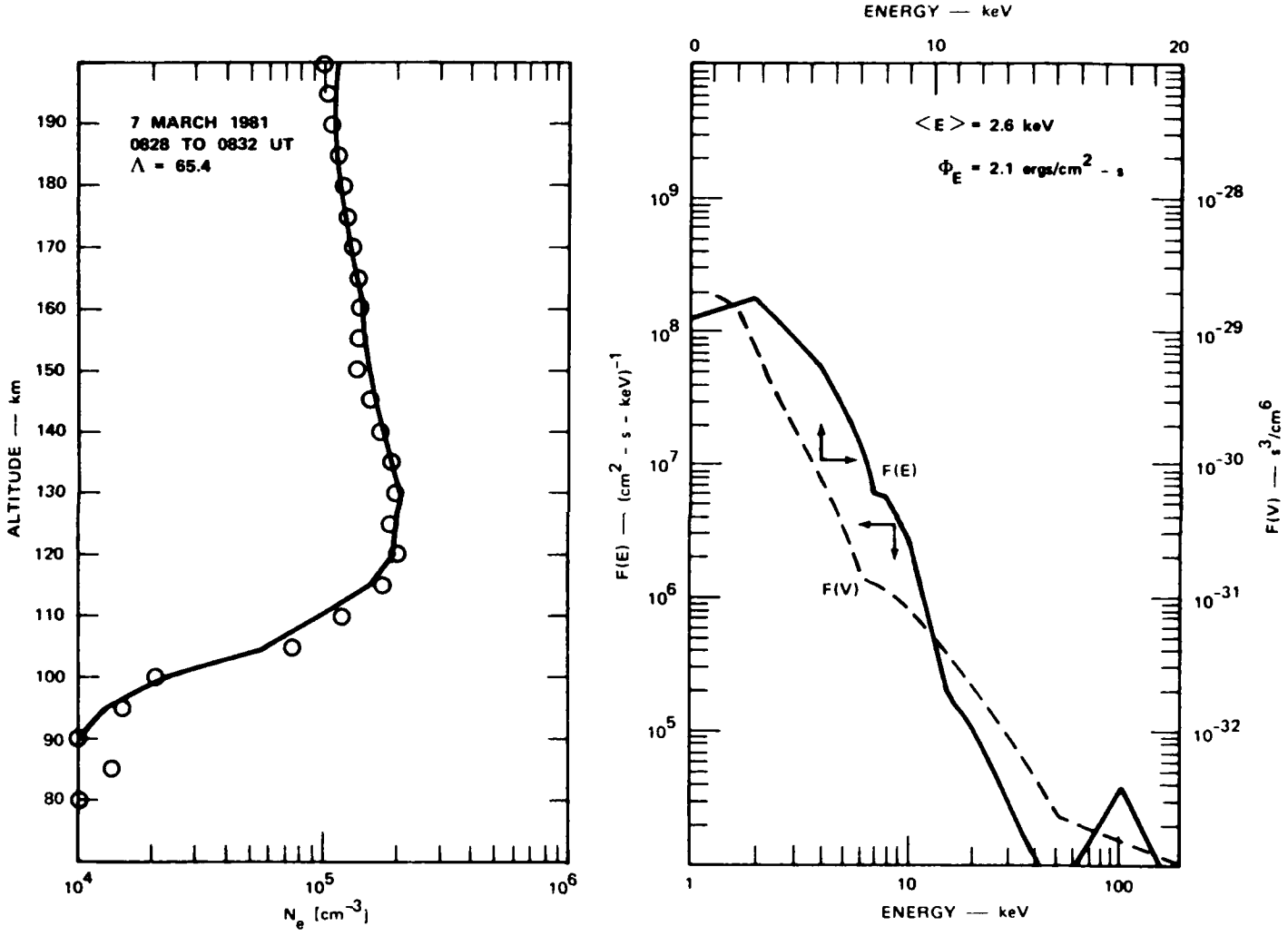

FIGURE 9 ELECTRON-ENERGY SPECTRUM DEDUCED FROM A FIELD-ALIGNED DENSITY PROFILE MEASURED BETWEEN 0816 AND 0820 UT

energy of about 15 keV. Above this energy the differential number flux is greater than expected from a Maxwellian. This high energy-tail on the distribution function is responsible for the extension of ionization to altitudes below 100 km as seen in the profiles. The mean energies are typical of plasma-sheet particles. The energy flux associated with the precipitation is 1.0 to 2.0 ergs/cm^2-s.

An alternative method for deducing the characteristics of the precipitating particles is to compute the height-integrated Hall and Pedersen conductivities from the measured density profiles. The grid lines in Figure 10 give the number density and characteristic energy of a Maxwellian electron source required to produce different values of the height-integrated Hall and Pedersen conductivity. The data points in the figure show the conductivity values computed from radar density measurements during the auroral-E experiment. The ionization in the diffuse aurora can be attributed to a source of density 0.4/cm^3 but with characteristic energies varying between 0.8 and 1.6 keV (mean energies between 1.6 and 3.2 keV). The resulting energy flux is given by

$$E[\text{ergs/cm}^{-2}\text{-s}] = 1.69\ N_o\ \alpha^{3/2}$$

where N_o is the density in cm^{-3} and α is the characteristic energy in keV. Thus, the energy flux in the diffuse aurora varied between 0.5 and 1.4 ergs/cm^2-s. The advantage of displaying the data in this manner is that trends in the data stand out more clearly. In particular, Figure 10 shows that the change in flux in the diffuse aurora resulted primarily from variations in the temperature of the source, not the density.

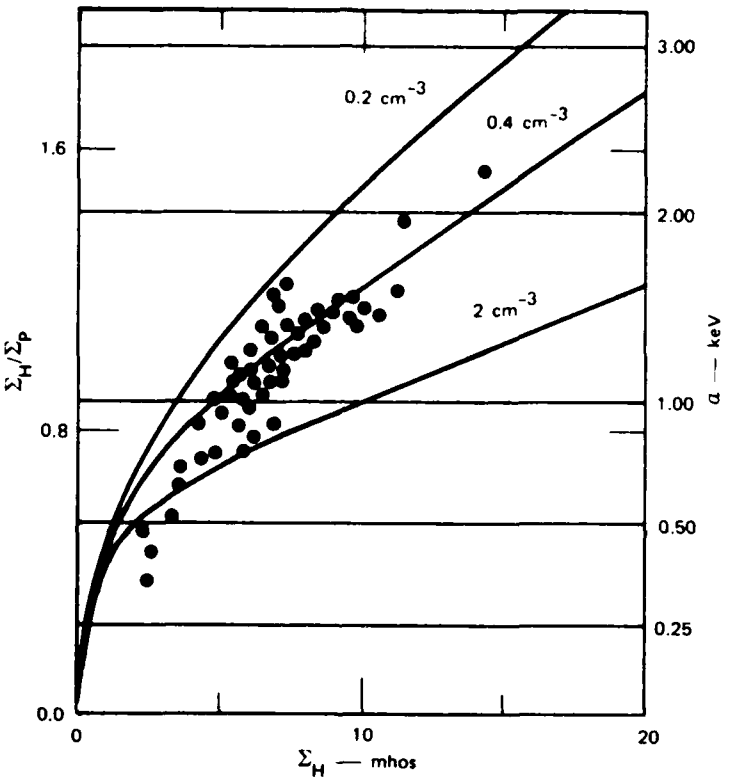

FIGURE 10 SCATTERPLOT OF HEIGHT-INTEGRATED HALL AND PEDERSEN CONDUCTIVITIES COMPUTED FROM THE ELECTRON DENSITY MEASUREMENTS MADE DURING THE SEVEN PARTIAL MERIDIAN SCANS OF FIGURE 2. Grid lines give the density and characteristic energy of a Maxwellian source required to produce the measured conductivities.

IV COMPARISON WITH ROCKET-BORNE INSTRUMENTATION

A. Pulsed-Plasma Probe

The dashed curve in Figure 5 shows the electron temperature measured by the pulsed-plasma probe during the flight of Payload A13.020 (D. Walker, private communication). The measurements are 200° to 400° higher than that measured by the radar. However, the radar measurements were made between 0849 and 0909 UT, whereas Payload A13.020 was in flight between 0810 and 0818 UT. The magnitude of the electric field at the time of the radar temperature measurements was about 30 mV/m (Robinson and Vondrak, 1981) compared to 50 mV/m during the first pair of rocket launches (Figure 4). This difference in electric field may account for the discrepancy in Figure 5. To estimate the electron temperature before the radar measurements, we note that the ion temperature above 160 km is given by Banks and Kockarts (1973) as:

$$T_i = T_n + 1217\ (E_\perp/55)^2$$

where T_n is the neutral temperature and $E_\perp$ is the magnitude of the electric field. Thus, using T_i from Figure 5 and using $E_\perp$ = 30 mV/m, the neutral temperature at 200 km is about 950°. This neutral temperature is consistent with the 1000° thermopause model of Banks and Kockarts (1973). Using this same equation with $E_\perp$ = 50 mV/m gives an ion temperature at 200 km of about 1950°. This temperature is more consistent with the plasma probe results if it can be assumed that $T_e \approx T_i$.

Although the F-region ion and electron temperatures at the time of rocket launches may have been somewhat higher than that shown in Figure 5, the corrections that must be applied to the raw density measurements are not significantly different from those shown in Figure 6 because the electron-to-ion temperature ratio in either case does not differ substantially from unity. The radar data does not indicate that the ion and electron temperatures were significantly different. However, the

electron temperature may have been enhanced in a thin layer. Such an enhancement would be undetectable by the radar because of altitude smearing over the 96 km range gate. Ennanced electron temperatures at about 115 km have been observed by Schlegel and St.-Maurice (1981). This enhancement was attributed to heating from unstable plasma waves generated in the presence of large electric fields (St.-Maurice et al., 1981). The 50-mV/m electric fields observed during the auroral-E experiment were above the threshold necessary for the generation of these waves. In addition, preliminary examination of the AC electric-field data indicated the existence of a turbulent region from 95- to 106-km altitude (M. Smiddy, private communication). If $T_e/T_i \approx 2$ in the turbulent layer a 50-percent correction to the raw densities would have to be applied. However, no enhanced electron temperature is apparent in the plasma probe data, which begin at 116 km. Even if such a correction was applied to the raw density profile, it would not change the density at the E-region peak, which was well above the turbulent region.

The electron density measured by the plasma probe is shown by the dashed line in Figures 3 and 6. They were systematically higher than the radar measurements at all altitudes. Figure 3 shows that the spatial and temporal variations in the diffuse aurora were not large enough to account for this discrepancy. Also, Figure 6 shows that the temperature corrections were not large enough to bring the measurements into agreement, although the corrections were in the right sense. Other plasma probe-radar comparisons have produced similar discrepancies (V. Wickwar, private communication).

B. Ion-Mass Spectrometer

The fractional abundances of O^+ measured during the flight of Payload A13.020 by Swider and Narcisi (1981) were less than the quiet day values given by Kelly and Wickwar (1981). This depletion may be due to an increase in the charge exchange reaction $O^+ + N_2 \rightarrow NO^+ + N$. This increase results from enhanced N_2 concentrations caused by heating of the neutral atmosphere by ion-neutral collisions during times of intense Joule heating. The reaction rate for the above reaction is also

increased when the ion temperature is enhanced. The high electric fields and large ion temperatures during the auroral-E rocket flights are consistent with the presence of significant Joule heating. Neglecting neutral winds the Joule heating rate is given by $\Sigma\ pE^2$ where Σ p is the height-integrated Pedersen conductivity. Taking Σ_p = 7 mhos and E = 40 mV/m gives a Joule heating rate of about 1 erg/cm^2-s. This is comparable to the energy input from precipitating electrons in the diffuse aurora.

C. Electric-Field Booms

The electric-field probe on Payload A10.903 measured a DC electric field of 30 to 40 mV/m (M. Smiddy, private communication). The last scan in Figure 4 shows that the radar also measured electric fields within these limits at about the same time. The good agreement between the two measurements indicates that the E-region neutral wind was small during the experiment. A wind of 100 m/s would produce a 5 mV/m error in the radar electric field. Because the radar and rocket electric-field measurements agree within this limit, the E-region neutral wind at the time of the experiment probably did not exceed 100 m/s.

V SUMMARY

The four auroral-E rockets were launched into a broad continuous aurora with peak E region densities of 1 to 2 x $10^5 cm^{-3}$. The altitude of the peak was between 120 and 125 km. Electric fields across the layer varied from 30 to 50 mV/m and were directed slightly west of north. The ion and electron temperatures were elevated over the neutrals because of Joule heating. The Joule heat input rate was about 1 erg/cm^2-s. This heating may have been responsible for the higher than average amount of molecular ions relative to O^+. The corrections to the raw electron densities measured by the radar were typically less than 20 percent because the electron-to-ion temperature ratio was close to one. Although the Langmuir probe AC electric-field data indicated the presence of a turbulent layer at about 100 km, no evidence of anomalous heating is present in the radar data or in the plasma probe data. However, this layer may have been low enough and thin enough to be undetectable by these instruments.

The ionization in the continuous aurora was produced by precipitating electrons with average energies of about 2 keV and fluxes of 0.5 to 1.5 erg/cm^2-s. This flux was attributed to a source of electrons in the magnetosphere with a density of 0.4 cm^{-3} but with characteristic energies that varied between 0.8 and 1.6 keV.

REFERENCES

Banks, P. M. and G. Kockarts, Aeronomy, pp. 311-338 (Academic Press, New York, NY, 1973).

Kelly, J. D. and V. B. Wickwar "Radar Measurements of High-Latitude Ion Composition Between 140- and 300-km Altitude" J. Geophys. Res. Vol. 86, pp. 7617-7626 (1981).

Robinson, R. M. and R. R. Vondrak, "Chatanika Radar Measurements during the Auroral E Program," Scientific Report No. 1, Contract AFGL-TR-81-0238, SRI Project 273H, SRI International, Menlo Park, CA (June, 1981).

Schlegel, K. and J. P. St.-Maurice, "Anomalous Heating of the Polar E-Region by Unstable Plasma Waves. 1. Observations," J. Geophys. Res. Vol. 86, pp. 1447-1452 (1981).

St.-Maurice, J. P., K. Schlegel, and P. M. Banks, "Anomalous Heating of the Polar E-Region by Unstable Plasma Waves. 2. Theory," J. Geophys. Res., Vol. 86, pp. 1453-1462 (1981).

Swider, W., and R. S. Narcisi, "Problems with the $N_2^+ + O \rightarrow NO^+ + N$ Reaction in Aurora," Geophys. Res. Lett., Vol. 8, pp. 1239-1241 (1981).

Vondrak, R. R., and M. J. Baron, "A Method of Obtaining the Energy Distribution of Auroral Electrons from Incoherent Scatter Energy Measurements," Radar Probing of the Auroral Plasma Proceedings of the EISCAT Summer School, Tromso, Norway, June 5-13, 1975, A. Brekke, ed., pp. 315-330, (Universitetsforlaget, Tromso-Oslo-Bergen, 1977).